HSL, Harpur Hill
Buxton, SK17 9JN
Tel. 01298 218000
Fax. 01298 218590

HEALTH & SAFETY LABORATORY

Post Hatfield Rolling Contact Fatigue

Modelling of Bending Stresses in Rails

MM/04/29

Project Leader: **James Hobbs**
Author(s): **James Hobbs, PhD**
Science Group: **Engineering Control Group**

OFFICE OF RAIL REGULATION

DISTRIBUTION

Dr D Hoddinott (3)	RI TD (Authorising Officer)
Dr N G West	HSL Operations Director
Mr P F Heyes	Engineering Control Group, HSL
Prof J Beynon	University of Sheffield
Dr M Frolish	University of Sheffield
Prof A Kapoor	University of Newcastle
Dr D Fletcher	University of Newcastle
Dr J W Hobbs	HSL
Group Circulation (4)	HSL

Section File
Registry File

LIS (2)

PRIVACY MARKING:

Not to be communicated outside HSE without the approval of the Authorising Officer.

HSL report approval:	Dr W Geary
Date of issue:	November 2004
Job number:	JR31086
Registry file:	MM/PR/21
Electronic filename:	H:\Work\HSE\Research\JR31086 - RCF\bending_report.doc

CONTENTS

EXECUTIVE SUMMARY

Objectives

The current report is part of an ongoing investigation into the phenomenon of rolling contact fatigue in rails. HSE is funding a two-year programme, which focuses on:

a) A three dimensional assessment of the crack morphology observed in head hardened rail.
b) The cause of crack branching (using whole-life model).
c) The role of residual stress in the development of rolling contact fatigue cracks.
d) The influence of pro-eutectoid ferrite and decarburisation on crack growth.

Presented here is the work carried out to model the bending induced in a rail, and its effect on the stress intensity factors associated with cracks in the rail head.

Main Findings

1. A significant length of rail is required in the model to obtain the correct level of constraint for the rail. Positioning a loading point close to the end of the rail model results in higher bending stresses and deflections.

2. The highest positive bending stress in the rail head occurs when the wheel loads are equidistant from the location of the crack, under normal loads and sleeper stiffnesses.

3. The stiffness of the sleeper supports has an effect of the bending stresses in the rail. Softer supports increase the stress while firmer supports reduce the stress.

4. Under the bending stresses alone, the tendency is for cracks to turn down into the head of the rail, for all crack depths and angles analysed.

5. High negative mode I stress intensity factors occur for cracks in the rail head when the load is directly over the crack. More work needs to be done on combining bending stresses with contact stresses and residual stresses to determine the effect of these negative SIFs.

Recommendations

The combined effect of bending, contact and residual stresses should be evaluated, as the effect of negative mode I stress intensity factors is not known.

1 INTRODUCTION

In order to investigate the phenomenon of rolling contact fatigue in rails, HSE is currently sponsoring work specifically on head hardened rail, focusing on:

a) A three dimensional assessment of the crack morphology observed in head hardened rail.
b) The cause of crack branching (using whole-life model).
c) The role of residual stress in the development of rolling contact fatigue cracks.
d) The influence of pro-eutectoid ferrite and decarburisation on crack growth.

This report details the modelling of bending stresses in rails due to wheel loads and the effect on crack growth. The bending stress is one of three main stresses acting on the rail head, the other two being contract stresses and residual stresses. The effect of the other stresses is addressed in other reports in this programme.

By evaluating the stresses, and calculating crack growth rates and estimating directions of growth, a better understanding can be obtained of the conditions under which cracks turn down and grow into the rail.

2 BOUNDARY ELEMENT MODEL

2.1 GEOMETRY, LOADING AND CONSTRAINTS

The profile of the rail is shown in Figure 1, with the meshing areas (patches) used for the zone boundaries (internal lines). Each length of rail was spit into three zones; the head, the web and the foot. BEASY, the boundary element software used for this work, uses zones to reduce the size of the working files and maintain a good quality of solution. Zones should not have excessive aspect ratios, so the length of the rail was also split into a number of zones, limiting the length of each zone to a maximum of one sleeper spacing (650 mm). There were a total of 48 zones used in the model.

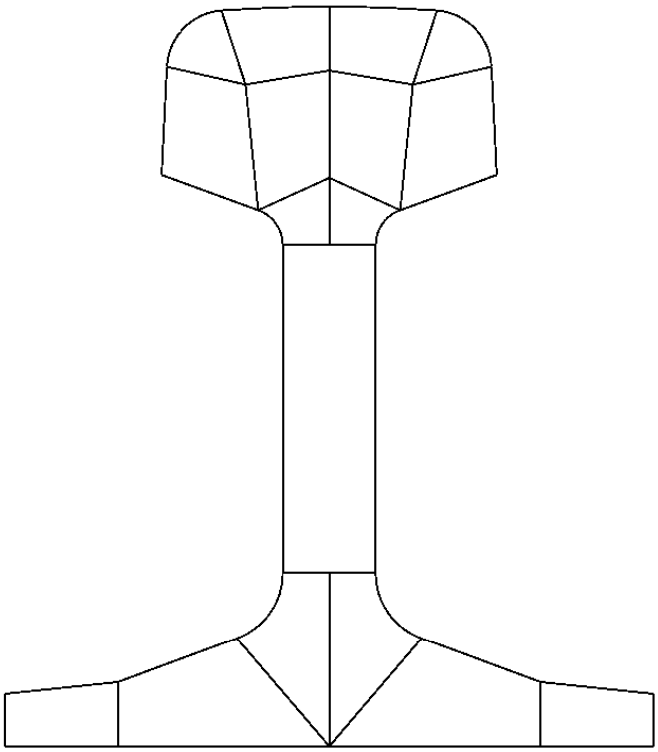

Figure 1 Profile of rail. Internal lines indicate separate meshing areas (patches) used in the model.

The main constraints applied to the rail represented the support from the sleepers. The constraints were applied in the form of springs applied to the bottom of the rail foot with a stiffness defined in the vertical direction only. The stiffness of the sleepers was taken from a paper by Dukkipari and Dong [1] and was approximately 40MN/m. As springs in BEASY use pressure, rather than force, per unit displacement, this value equated to 2.86 MPa/mm, since the area of the rail foot supported by each sleeper was approximately 0.014 m^2. The displacement of the foot was also constrained in the lateral direction by applying displacement constraints to an element on the side of the rail foot adjacent to the sleeper. The spacing of the sleepers was 650 mm, with a width of 100 mm. A schematic diagram of the whole rail model is shown in Figure 2.

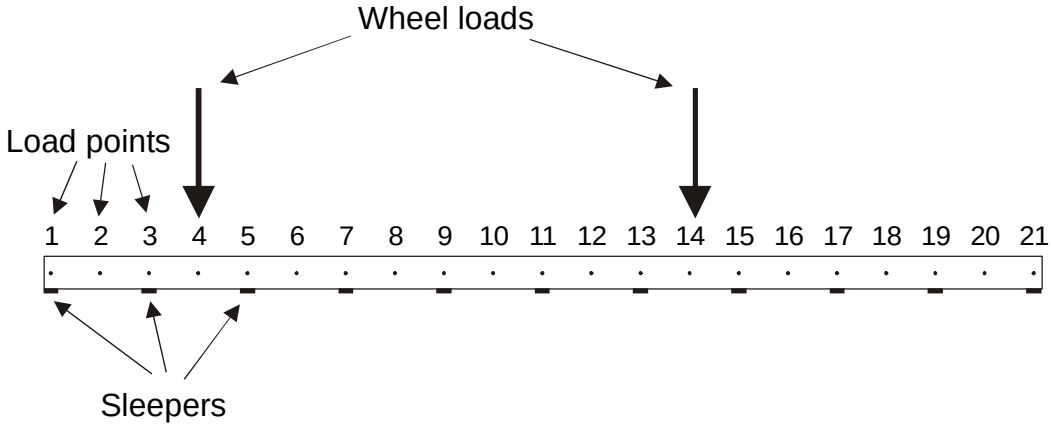

Figure 2 Schematic diagram of the rail model showing sleepers and loading points. Wheel loads are shown

Loads were applied using point loads located in the centre of the web at various positions along the length of the rail. The loading points were positioned at mid span points between sleepers and centrally over sleepers, as shown in Figure 2. Models were run with the load appropriate for a wheel on a power car (i.e. 10 tons per wheel) applied to each loading point in turn. When the first load was applied to loading point 11, a distance of 3.25 m from the first loading point, a second load, again that appropriate for a wheel on a power car, was applied to the first loading point. This distance was approximately equivalent to the distance between the two wheel centres on one powercar bogie. From this stage, the two loads were moved together, keeping a bogie length spacing between the loads.

A crack was added to the model above the sleeper at load point 9. Figure 2 shows the case where the two wheel loads are located at points 4 and 14, with the crack directly in the middle.

It should be noted that as the loads were applied to the web, the stress intensity factors obtained at the crack tip take no account of the contact force on the rail head that would have been applied in real life. This model is only intended to show the results from the bending of the rail. Another limitation of this model is that it is static, and does not replicate the dynamic forces generated as wheels pass over the rail at high speed.

3 RESULTS & DISCUSSION

3.1 UNCRACKED MODEL

A model was run without a crack, but with the wheel loads equidistant from the position at which the crack would later be added, i.e. loads at points 4 and 14. The results from this model are listed in Table 1. The areas of highest stress were located on the underside the rail foot beneath the loading points and on the top of the rail head at point 9.

The deflection and stress at the two loading points were not the same, with approximately a 10% difference for both deflection and stress. This is likely to be due to the fact the load point 4 was close to the end of the rail model and was therefore less restrained despite spring restraints being applied to the end of the rail in the longitudinal and vertical directions in an attempt to provide extra constraint.

	Maximum principal stress (MPa)	Maximum vertical deflection (mm)
Point 4 (left wheel)	82.0	-1.28
Point 9 (between wheels)	22.6	-0.067
Point 14 (right wheel)	74.5	-1.15

Table 1 Deflection and stress results for rail model without crack

A second model was run, taking advantage of the longitudinal symmetry present in the rail. This had the effect of moving the loading point further away from the end of the rail and therefore reduced the effects due to the lack of constraint at the ends of the model. The loading point was 7.5 sleeper spacings away from the end of the model in this case, as opposed to 1.5 and 3.5 spacings for the previous model. Contours of maximum principal stress are shown on the deformed rail in Figure 3, with the deformation exaggerated.

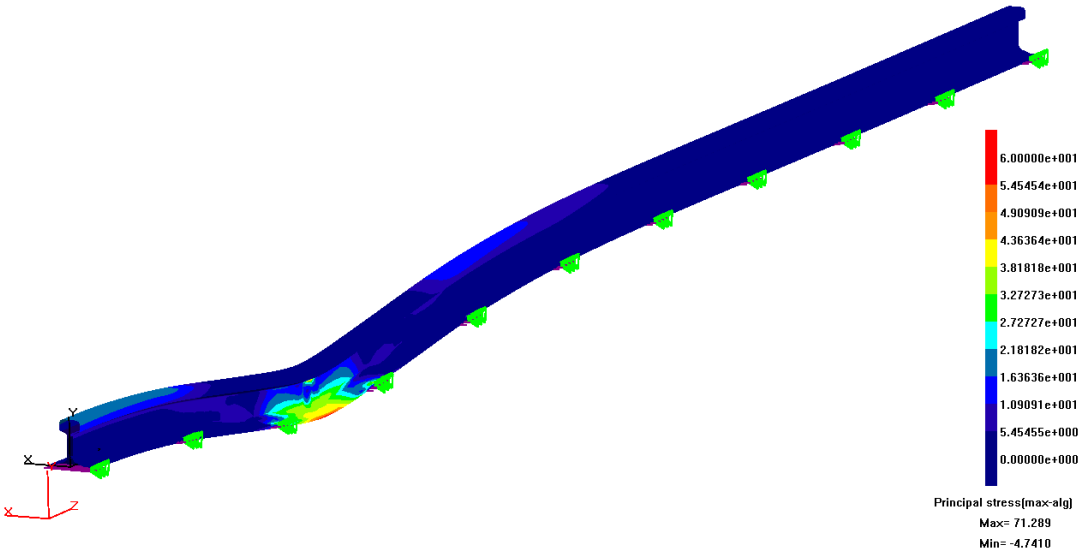

Figure 3 Contours of maximum principal stress for symmetrical rail model

The extra constraint achieved by keeping the load point further away from the ends of the model reduced the deflections and stresses in the rail. The stresses reduced to 71.2 MPa in the rail foot under the load and 20.8 MPa in the rail head between the loads. Deflections below the load reduced to -1.12 mm under the load but the deflection of the head between the loads remained largely unchanged at -0.068 mm.

The results from the symmetrical model are likely to be more accurate than the results from the standard model, with loads applied at load points 4 and 14, because of the effective extra length of the rail. However, as the cracks modelled were inclined they were not symmetrical in the longitudinal direction, so it was not possible to take advantage of the longitudinal symmetry for the models containing cracks. It would have been possible to extend the model, to increase the distance from the model ends, but this would have significantly increased the size of the model, resulting in longer run times.

For the purposes of the models containing cracks, it is the maximum stress in the head of the rail that is important. The standard model, with loads applied at load points 4 and 14, overestimated this stress by approximately 10%, compared to the symmetrical model. This should be borne in mind when looking at the SIF results, although the relationships between mode I and mode II SIFs, and the effect of varying different parameters should still be valid.

It is clear from the results that the highest bending stresses occur in the foot of the rail when the wheel is directly above. The stresses in this case were more than 3 times higher than the highest stress in the head of the rail. The fact that cracking in the rail head, rather than the foot, is a problem indicates the importance of other mechanisms, i.e. the effect of contact, on the initiation and initial propagation of cracks.

3.2 CRACKED MODELS

3.2.1 Position of crack relative to wheels and sleepers

The effect of applying the load at different positions is shown in Figure 4. The figure shows K_I stress intensity factor for a semi-circular crack of length 10 mm and inclination of 30°, positioned over the sleeper at loading position 9.

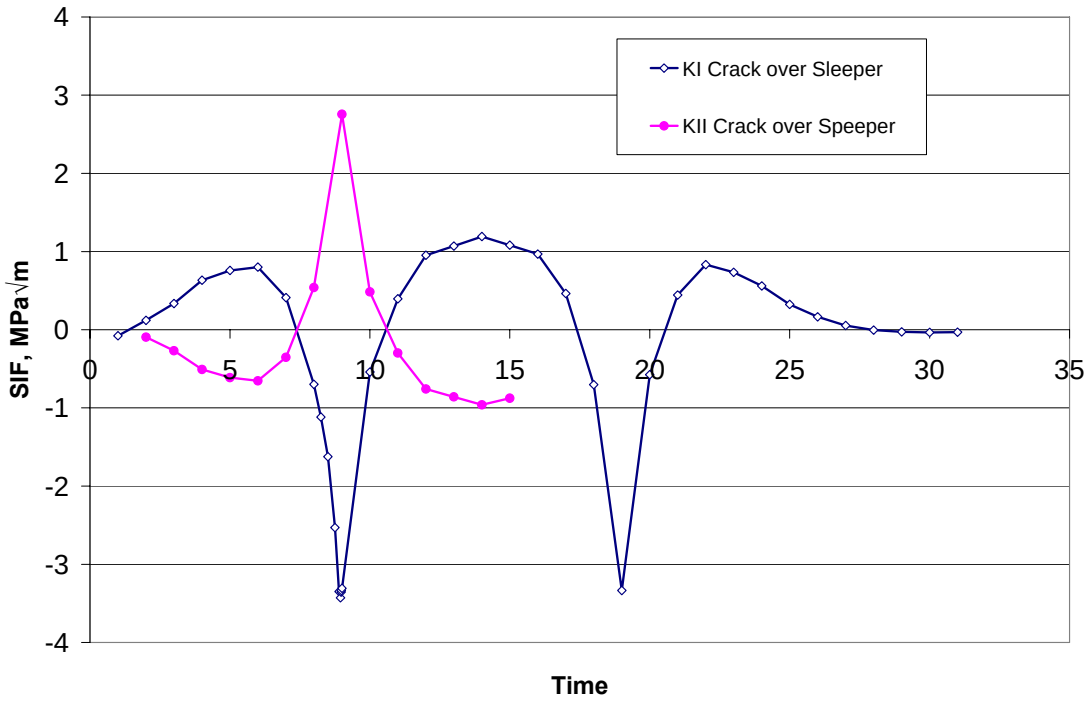

Figure 4 Mode I and mode II SIFs for a crack in a rail with loading wheels at different positions

As the wheel approaches the crack location, the stress intensity factor at the crack tip increases until point 6, 1.5 sleeper spans from the crack tip. As the wheel gets closer still to the crack, the SIF values decrease and become large and negative as the wheel passes over the crack. A negative mode I SIF indicates that crack closure would have taken place; in reality the faces of the crack would come into contact and the crack would not experience a negative SIF, but would stay at zero. The range of stress intensity factors experienced at the crack tip over the loading cycle would just be the positive SIF range from zero to the maximum. However, the action of other stresses acting on the rail, namely, the contact stresses and residual stresses, may act to increase the overall stress. This could lead to crack closure being delayed and the overall range of SIFs increasing over the cycle. More work needs to be done to combine the different stresses to determine the overall stress cycle.

The highest positive mode I SIF occurs with a wheel at either side of the crack, when the first wheel is at position 14 and the second wheel is at position 4. It is the stress in this position that is most likely to provide a driving force for crack growth as the bending in this position acts to open the crack. At this position, the mode II SIF are negative. The sign convention used was that negative mode II SIFs tend to turn the crack down, further into the head of the rail.

All the above results are for a crack positioned above a sleeper. The effect of positioning a crack mid-way between sleepers was also investigated. The results can be seen in Figure 5, alongside those for a crack above a sleeper.

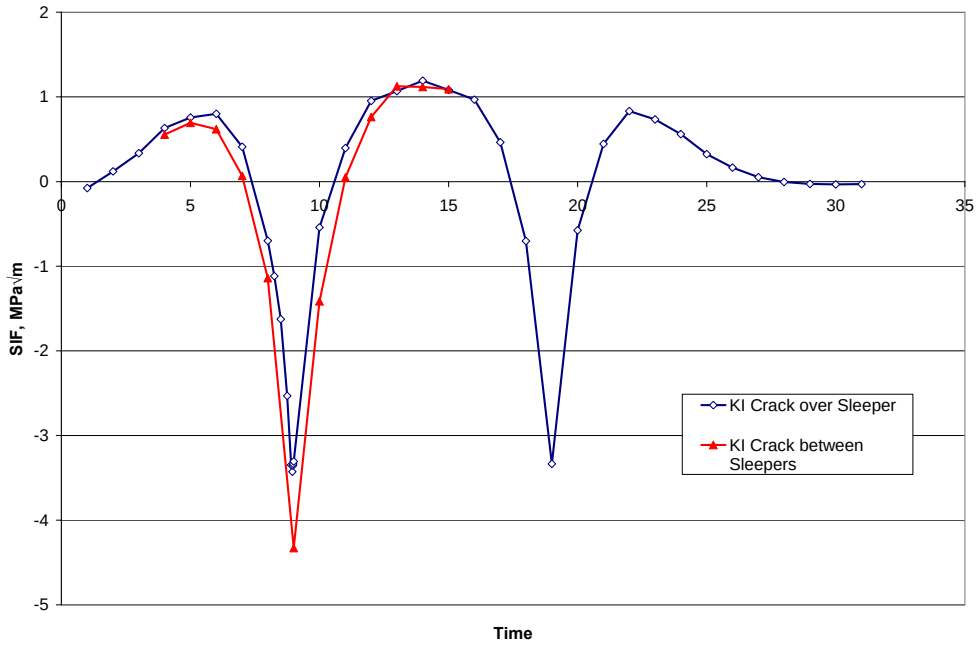

Figure 5 SIFs for different crack positions in relation to sleeper support

As can be seen from Figure 5 the largest difference due to the placement of the crack occurs when the wheel is situated above the crack. The magnitude of the SIF increases by approximately 26%. For this case, but at this point the SIF is negative and therefore it is likely that the crack would be closed and that this SIF would not actually be experienced at the crack tip.

For the case of the highest positive mode I SIF, when the crack is between the two wheel loads, the position of the crack relative to the sleeper support does not have a significant effect, only reducing the SIF by 5%. It is unlikely that the growth of cracks would vary significantly with position relative to sleeper support, due to the difference in bending stress.

3.2.2 Effect of different supports

The effect of different supports was also investigated. In addition to the standard sleeper support taken from Dukkipari and Dong [1], a softer sleeper was modelled and a continuous support. For the continuous support, the stiffness assumed was that of the standard sleeper, applied along the continuous full length of the rail. As the standard model used sleepers with a width of 100 mm and spacing of 650 mm, the overall stiffness using the continuous support was 6.5 times that of the standard model. The softer sleeper support has a stiffness of half that of the standard sleeper.

The effect of changing the rail support is shown in Figure 6. The effect of reducing the stiffness was to increase the bending in the rail by almost 50%. Having a continuous bed, and therefore generally a stiffer support, had the effect of reducing the maximum bending stress to approximately one third of the original value. Also, the location of the wheels relative to the crack at the point of highest bending stress changes. The highest stress no longer occurs when the crack is positioned centrally between the two wheels but now occurs when a wheel is closer to the crack. The extra stiffness obtained by using the using continuous supports limits the

range of effect of the wheel loads, with the stress levels falling quickly after the wheel passes. It is likely that this effect is due to the overall increase in support stiffness, rather than the fact that the support was continuous.

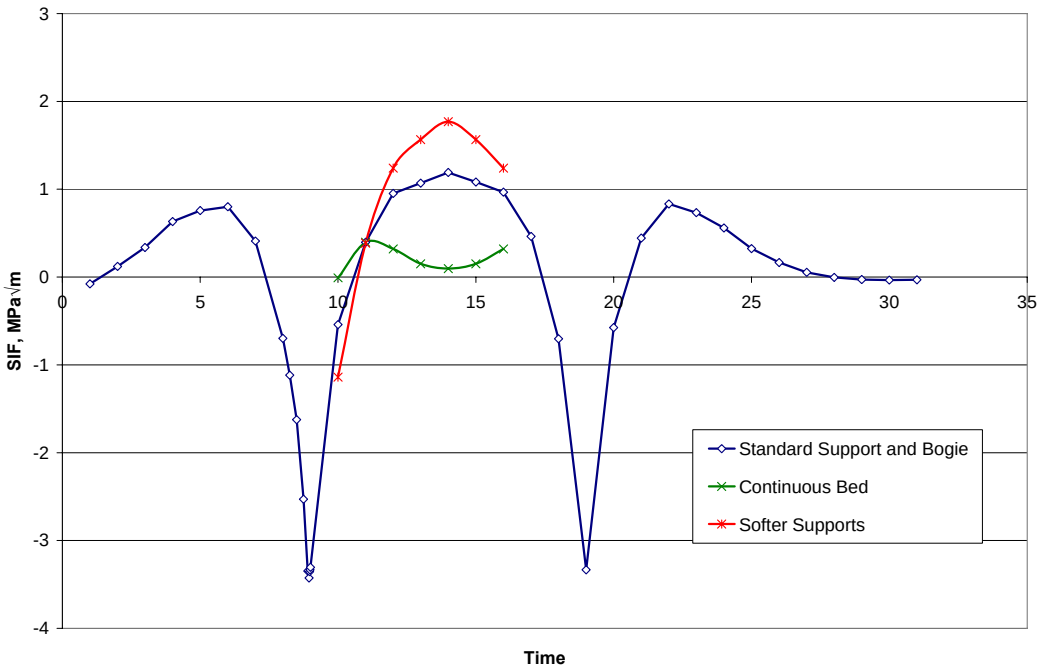

Figure 6 Effect of changing rail supports

3.2.3 Effect of Different Crack Parameters

The effect of different crack depths and angles is shown in Figure 7 and Figure 8. In all cases, the cracks were positioned above a sleeper, with the loading point equidistant from the crack (loads at points 4 and 14). Figure 7 shows the SIFs in terms of the crack lengths, measured from the crack mouth to the crack tip. Figure 8 shows the SIFs in terms of the crack depth, i.e. the vertical distance of the deepest point of the crack tip from the head of the rail.

The mode I SIFs for a 45° crack were higher than for the 30° crack when compared by crack length or by crack depth. However, mode II SIFs were found to be affected only slightly by crack angle.

The sign of the mode II SIFs indicate that the cracks would turn down and grow at a steeper angle into the rail head. The ratio of mode I to mode II SIFs was higher for the 45° cracks, indicating that there was a smaller tendency for the crack to turn down. For the 30° crack, the magnitude of the mode I SIF exceeded that of the mode II SIF by approximately 15%, whereas this figure was approximately 50% for the 45° crack.

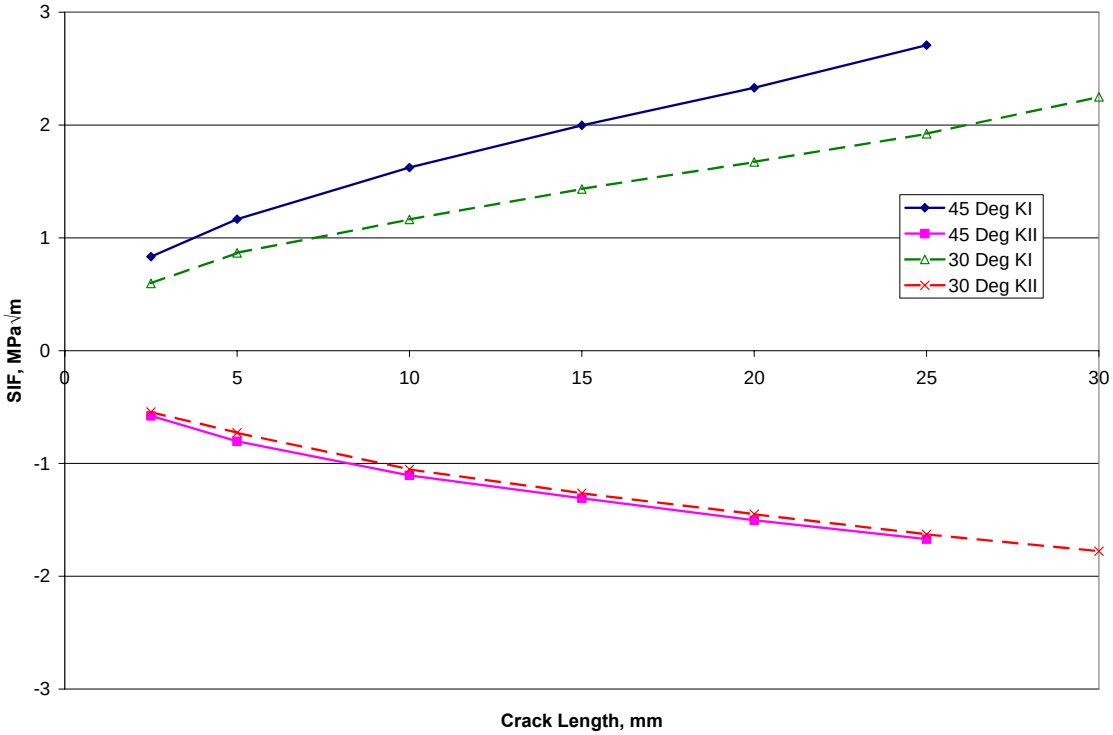

Figure 7 Variation of SIFs for 30° and 45° crack in terms of crack length

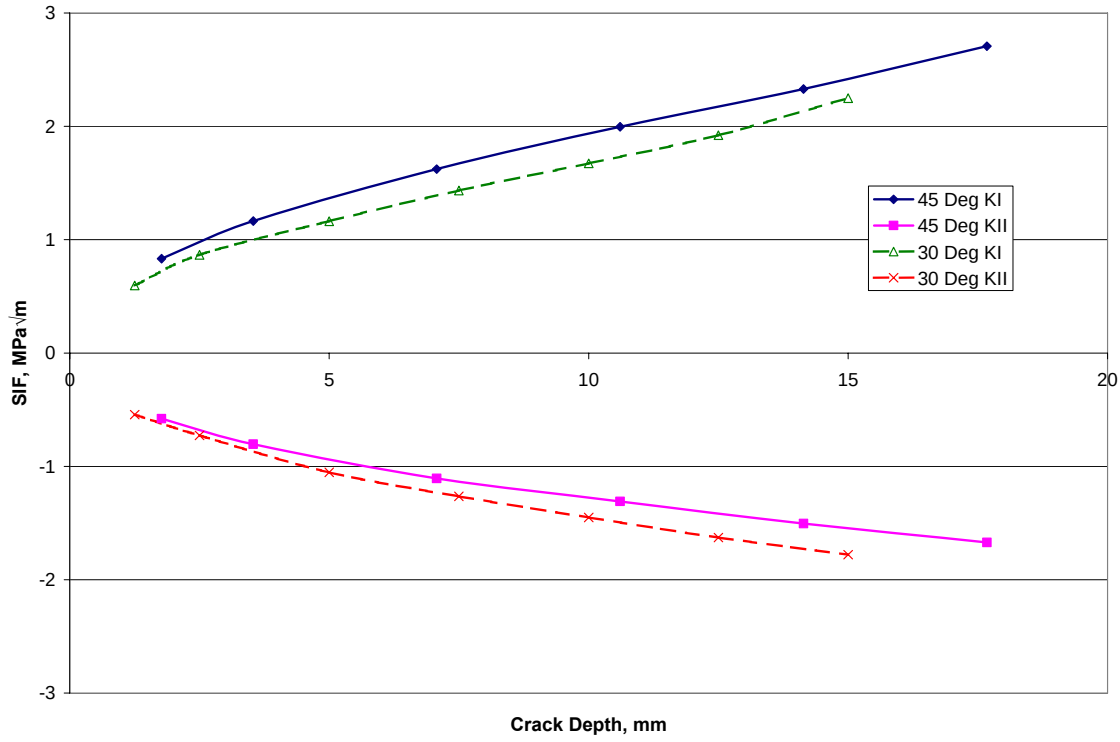

Figure 8 Variation of SIFs for 30° and 45° crack in terms of maximum crack depth

4 CONCLUSIONS

1. A significant length of rail is required in the model to obtain the correct level of constraint for the rail. Positioning a loading point close to the end of the rail model results in higher bending stresses and deflections.

2. The highest positive bending stress in the rail head occurs when the wheel loads are equidistant from the location of the crack, under normal loads and sleeper stiffnesses.

3. The stiffness of the sleeper supports has an effect of the bending stresses in the rail. Softer supports increase the stress while firmer supports reduce the stress.

4. Under the bending stresses alone, the tendency is for cracks to turn down into the head of the rail, for all crack depths and angles analysed.

5. High negative mode I stress intensity factors occur for cracks in the rail head when the load is directly over the crack. More work needs to be done on combining bending stresses with contact stresses and residual stresses to determine the effect of these negative SIFs.

5 REFERENCES

[1] Dukkipati, R.V. and Dong, R. Idealized steady state interaction between railway vehicle and track, *Proc Instn Mech Engrs Part F*, 1999, Vol 213, 15-29.